Ernst-Moritz-Arndt University of
Greifswald

Master Thesis

Kinetic effects in RF discharges

Author:
Philipp Hacker

Supervisor:
Prof. Dr. Ralf Schneider

*A thesis submitted in fulfillment of the requirements
for the degree of Master of Science - Physics*

in the research group of

Computational Sciences,
Institute of Physics

July 31, 2017

"Without encroaching upon grounds appertaining to the theologian and the philosopher, the domain of natural sciences is surely broad enough to satisfy the wildest ambition of its devotees. [...] The work may be hard, and the discipline severe; but the interest never fails, and great is the privilege of achievement. "

— John William Strutt, 3rd Baron Rayleigh, 1884
in: Address to the British Association in Montreal

Declaration of Authorship

I hereby certify that this thesis has been composed by me and is based on my own work, unless stated otherwise. No other person's work has been used without due acknowledgement in this thesis. All references and verbatim extracts have been quoted, and iall sources of information, including graphs and data sets, have been specifically acknowledged.

.....
Signature of author
Greifswald; July 31, 2017

Contents

List of Abbreviations

abbreviation	full expression
e.g.	exempli gratia; *for example*
etc.	et cetera; *and so on*
ac	alternating current
dc	direct current
rf	radio frequency
ccrf	capacitively coupled radio frequency

Table 1: List of abbreviations and their corresponding phrases. If specified, the translation or an equivalent expression is written.

Physical Quantities

Quantity	Unit	Symbol	Dimension	Value
Speed of Light	m/s	c_0		$2{,}997 \cdot 10^{8}$
Vacuum permittivity	F/m	ε_0	$\mathrm{s^4A^2m^{-3}kg^{-1}}$	$8{,}854 \cdot 10^{-12}$
Boltzmann constant	eV/K	k_B	$\mathrm{JK^{-1}}$	$8{,}617 \cdot 10^{-23}$
planck constant	eVs	$\hbar$	$\mathrm{m^2kg\,s^{-1}}$	$4{,}1345 \cdot 10^{-15}\,\mathrm{eVs}$ $6{,}646 \cdot 10^{-34}\,\mathrm{Js}$
particle mass	kg	m_j		electron: $9{,}109 \cdot 10^{-31}$ ion: $5{,}310 \cdot 10^{-26}$ anion: $5{,}143 \cdot 10^{-26}$
kinetic temperature	eV	T_j	K	$1\,\mathrm{eV} = 1{,}902 \cdot 10^{-19}\,\mathrm{K}$
elementary charge	C	e	As	$1{,}902 \cdot 10^{-19}$
reduced mass	kg	$\mu_\mathrm{j,k}$		$(1/m_\mathrm{j} + 1/m_\mathrm{k})^{-1}$
particle density	$\mathrm{cm^{-3}}$	n_j	$\mathrm{m^{-3}}$	
Debye length	cm	$\lambda_\mathrm{D,j}$	m	
plasma frequency	Hz	$\omega_\mathrm{p,j}$	$\mathrm{s^{-1}}$	
thermal velocity	m/s	$v_\mathrm{th,j}$		
collisional frequency	Hz	ν_j	$\mathrm{s^{-1}}$	
particle distance	cm	$\overline{b}$	m	
mean free path	cm	$s_\mathrm{mfp,j}$	m	
electrostatic potential	V	Φ,U	$\mathrm{kg\,m^2A^{-1}s^{-3}}$	
mobility		μ_j		

Table 2: Physical properties in their commonly — or for this purpose most convinient — units and corresponding SI units. If not specified, the values of each quantity refer to the afore-mentioned units.

Abstract

The Thesis Abstract is written here and usually kept to just this page. The page is kept centered vertically so it can expand into the blank space above the title too.

Physical properties of low temperature RF plasma

In this first chapter I will provide the necessary physical background for this work about the numerical simulation of low temperature capacitively coupled radio frequency plasma. Here both the mathematical basics and method for the simulation, as well as the most important aspects about the plasma properties will be explained.

1.1 Plasma physics

1.1.1 Capacitively coupled radio frequency plasma

The experiment where after the conducted simulations is modelled after revolves around a capacitively coupled radio frequency, low temperature plasma at low pressures of oxygen.
Here, I will refer to a plasma as an globally quasi-neutral gas, consisting of freely moving charges — e.g. electrons, positiviely and negatively ions — and neutral gas particles. The ratio between charged and neutral species defines the *degree of ionization*, which in this case is very low. The term of global neutrality emphasizes the purpose for different lenght scales inside the gas itself. Hence, the associated condition of neutrality by equal densities $n_\mathrm{e} = n_\mathrm{i}$ only is valid for areas larger than the so called *Debye sphere*. Inside this ball with a radius of λ_D, the *Debye length*, the afore-mentioned neutrality is not satisfied.
The creation of a plasma is accomplished by 2 parallel metal plates — the electrodes — where on at least one an AC signal at radio frequency is applied — this kind of experimental setup is among the most common, thus being used for basic but also in-depth studies of the afore-mentioned discharges. Here, a rf signal at exactly 13,56 MHz with an amplitude between 100–1000 V will be used — this corresponds to a wavelength of 22,11 m for the excitation. The use of external magnetic fields is not within the scope of this work — correspondingly, the experiment I will refer to also did not include $\vec{B}$-fields.
That said, a multitude of electric setups are possible, such as coated or grounded electrodes. Therefore, different regimes of operation ensue. For example, differently driven or shaped metal plates heavily influence the charge creation process inside the plasma. In summary, the electrodes, neutral gas and electric layout resemble a dielectric hindered plate capacitor. This simplification can be used to access important physical properties, such as an additional voltage offset on one of the electrodes or charge currents at such. A basic scheme of an asymmetric rf discharge can be seen in figure 1.1.

In the case of different electrode sizes, as seen in the scheme, the potential inside the spatially restricted area between wall and discharge can change drastically. This plasma sheath forms also between grounded parts of discharge containment or probes and plasma volume. This additional direct current offset is called *self-bias* (see section 1.1.4). A dielectric displacement current between plasma sheath and volume accomodates as a result of the different time scales of particle movement (see section 1.1.5). Especially, self-bias and displacement current play a key role in the following investigations, as a capacitive coupling between electrodes and power supply is difficult to model in a numerical kinetic simulation. In comparison to other low temperature, low pressure discharges — an example could be a dielectric hindered dc discharge at high voltages, with an electrode space gap of just a couple millimeters —, radio frequency plasma are characterized by their unique transport process inside the sheath and heating mechanisms of charged species. A more in-depth discussion can be found in section 1.1.6.

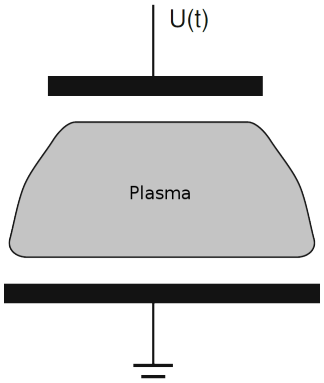

Figure 1.1: Schematic of an asymmetric discharge with one grounded and one driven electrode.The rf signal is denoted with $U(t)$.

1.1.2 Sheath physics and wall interaction

In the discharges bulk, neutral gas particles are exctited by electron collisions and radiating visible light. However, areas around, e.g. floating metal surfaces, probes and grounded walls are darker than the bulk. This is due to the low electron density and kinetic energy in this *plasma sheath*. Though areas with vanishing electron numbers can glow because of high collision efficiencies and/or frequencies.
Electrons, in general, are of a much higher mobility μ_e and thermal velocity $v_{\mathrm{th,e}}$. Hence they impinge onto walls and surfaces more often than other species, leading to a — in this case we consider an electronegative oxygen discharge, where the following can be assumed true — negative charge and potential.

Child-Langmuir Law

For an asymmetric ccrf discharge, DC *self bias* and displacement current are important parts of the electric system. Hence, the *Child-Langmuir Law* as a function of those properties can be written. The rf component of the excitation is neglected.
A greatly negative charged wall at $x = 0$ shall be a barrier for electrons of thermal velocity, e.g. $|\Phi(0) - \Phi(d)| \ll k_\mathrm{B}T_\mathrm{e}/e$. The thickness of the sheath shall be considered d. In an one-dimensional approach, the electron density $n_\mathrm{e}(x)$ can be written with a *Boltzmann* distribution function $f_\mathrm{B}(\Phi)$:

$$n_\mathrm{e}(x) = n_\mathrm{e}(d) \cdot f_\mathrm{B}(\Phi) = n_\mathrm{e}(d) \cdot \exp\left(\frac{e(\Phi(x) - \Phi(d))}{k_\mathrm{B}T_\mathrm{e}}\right) \quad . \tag{1.1}$$

This means that the electron density decreases exponentially towards the negatively charged wall. It can be assumed that the sheath thickness $d \ll s_{\mathrm{mfp,i}}$ the mean free path of the ions inside the plasma bulk. Hence, ions enter the sheath collisionless.
At the boundary between bulk and pre-sheath, the walls potential vanishes because of the plasmas shielding capabilities. Here, the ions are at $v_{\mathrm{i},0}$ speeds, therefore their density becomes:

$$n_{\mathrm{i}}(x) = n_{\mathrm{i}}(d)\left(1 - \frac{2e\Phi(x)}{m_{\mathrm{i}}v_{\mathrm{i},0}^2}\right)^{-1/2} \tag{1.2}$$

Futhermore, one can assume that the kinetic energy at this point is smaller than the potential energy for the acceleration inside the pre-sheath, e.g. $m_{\mathrm{i}}v_{\mathrm{i},0}^2 \ll |e\Phi(x)|$. Using *Poisson's* equation, and taking into account the ion-sheath interaction, equation 1.3 gives an equation for $\Phi(x)$:

$$\Delta\Phi \cong -\frac{en_{\mathrm{i}}\left(-d\right)}{\varepsilon_0}\left(-\frac{2e\Phi\left(x\right)}{m_{\mathrm{I}}v_{\mathrm{i},0}^2}\right)^{-\frac{1}{2}} \tag{1.3}$$

Solving this, and using the unpertubated ion current $j_{\mathrm{i}} = n_{\mathrm{i}}(d)ev_{\mathrm{i},0}$, one yields the result by *Langmuir*.

$$\Phi\left(x\right) = \left(\left(\frac{3}{4}\left(x+d\right)\right)^4\left(\frac{j_{\mathrm{i}}}{\varepsilon_0}\right)^2\frac{m_{\mathrm{i}}}{2e}\right)^{\frac{1}{3}} \tag{1.4}$$

Again, solving equation 1.4 for the current j_{i} yields the *Child-Langmuir Law* (see equation 1.5). This equation defines the ion current as a function of the unpertubated plasma bulk. In other words, the sheath changes its thickness in dependency of those certain discharge parameters, always satisfying the ion current defined by the *Child-Langmuir Law*.

$$j_{\mathrm{i}} = \frac{4}{9}\varepsilon_0\left(\frac{2e\left(\Phi\left(-d\right) - \Phi\left(0\right)\right)^3}{m_{\mathrm{i}}d^2}\right)^{\frac{1}{2}} \tag{1.5}$$

1.1.3 Bohm criteria

In section 1.1.2 the behaviour of charge particle densities inside the plasma sheath has been discussed. In contrast to the discharge volume, those densities do not satisfy the quasi-neutrality condition in a distance of d from the wall anymore. Though we know that the sheath is a spacially restricted area around electrostatic floating surfaces, a physical law concerning this circumstance has not been derived here. So the question ensues, why the area of electron depletion does not extend further into the discharge volume.
To answer this question, one has to take a look at a substitutional system. This will be a, likewise mechanical, one-body extremal problem of a point mass. In this case only kinematic

pontentials with inverted parabolic maxima are of interest. Therefore, in this unstable equilibrium, a small pertubation culminates into a large force on the test body.
To see the quality of this example, one has to take a look at the second order differential equation of the afore-mentioned mechanical problem and the electrostatic *Poisson's equation* (see equation 1.6).

$$m\frac{\mathrm{d}^2\vec{r}}{\mathrm{d}t^2} = -\frac{\mathrm{d}V}{\mathrm{d}\vec{r}} \quad \Leftrightarrow \quad \Delta_{\vec{r}}\Phi = -\frac{\mathrm{d}\Psi}{\mathrm{d}\Phi} = f(\Phi) \overset{\text{Poisson's}}{=} \frac{\rho}{\varepsilon_0} \tag{1.6}$$

For an instability, the force on the test body must increase with the distance from the equilibrium, hence the equation 1.8 is used to calculate the exact velocity at which an ion is entering the sheath. This results in the first *Bohm criteria*.

$$0 > \left.\frac{\mathrm{d}^2\Psi}{\mathrm{d}\Phi^2}\right|_{\Phi=0} \overset{\text{equation 1.6}}{=} \frac{\mathrm{d}}{\mathrm{d}\Phi}\left(\frac{n_\mathrm{e}(x) - n_\mathrm{i}(x)}{\varepsilon_0}\right)\Bigg|_{\Phi=0} \frac{en_\mathrm{e}(-d)}{\varepsilon_0}\left(\frac{e}{k_\mathrm{b}T_\mathrm{e}} - \frac{e}{m_\mathrm{i}v_{\mathrm{i},0}^2}\right) \tag{1.7}$$

$$\Rightarrow \quad v_{\mathrm{i},0} \geq v_{\mathrm{i,B}} = \sqrt{\frac{k_\mathrm{B}T_\mathrm{e}}{m_\mathrm{i}}} \tag{1.8}$$

Analoguos you can define the so called *Mach number* $M = v_{\mathrm{i},0}/v_{\mathrm{i,B}}$, where $v_{\mathrm{i,B}}$ denotes the *Bohm velocity*.
Now, to understand why the sheath does not extend further than a fixed distance d from the discharge boundary, the particle movement has to be investigated on a smaller scale. As seen above, there is an electric field in the *pre-sheath* that accelerates the ions to $v_{\mathrm{i,B}}$. In addition, quasi-neutrality is still satisfied here:

$$n_\mathrm{I}(x) = n_{\mathrm{I},0}\exp\left(\frac{e\Phi(x)}{k_\mathrm{B}T_\mathrm{e}}\right) = n_\mathrm{e}(x) \ . \tag{1.9}$$

Still, $\Phi(x)$ is the potential inside the pre-sheath from section 1.1.2 and $n_{\mathrm{i},0}$ the unpertubated density from the plasma *bulk*. A greater part of the ion transport process in this area is governed by collisions with neutral gas particles, hence the velocity distribution function with the collision frequency $\nu n, i$ has to be rewritten:

$$\frac{\mathrm{d}v_\mathrm{i}}{\mathrm{d}x} = \frac{\nu n, i v_\mathrm{i}^2}{v_\mathrm{B}^2 - v_\mathrm{i}^2} \quad . \tag{1.10}$$

From the singularity in equation 1.10 at $v_\mathrm{i} = v_\mathrm{B}$ and the knowledge of $\Phi(x)$ at the wall, one can calculate the sheath thickness d. Furthermore, ions with velocities smaller than the Bohm velocity are being accelerated inside the pre sheath. According to equation 1.8 velocities greater than v_B are not allowed here. This is, together with equation 1.10 the reason why the ion velocity is exactly v_B at the boundary of the plasma sheath and thus a positive space charge ensues.

$$M = 1 \Leftrightarrow v_{\mathrm{i}}(-d) = v_{\mathrm{B}} \tag{1.11}$$

Conclusively, at the sheath boundary equation 1.11 is satisfied.
At $x = -d$, both negative and positive charge density decreased to $n_{\mathrm{i}} = n_{\mathrm{e}} \approx 0{,}66 n_{\mathrm{e},0}$ — see **??** —, where the potential is approximately $-k_{\mathrm{B}} T_{\mathrm{e}}/2e$ because of the currents onto the wall.
In summerization, the plasma does not "see" its sheath, because the ion dynamic discussed before is spatially restricted. The sheath only develops where there is electron depletion or an externally applied, negative potential.

1.1.4 Self bias voltage

An important step towards the electric characterization of such ccrf discharges is the development of a replacement current, see **??**. Thus, one can define a specific impedance for a rf discharge of excitation frequency ω. The valeu of ε_{p} resembles the permeability of the working gas between the driven and/or grounded electrode. In addition, this volume has the capacity C_{p} — the capacity of a cubicle with a cross section A, thickness b and electron-neutral collision frequency $\nu_{\mathrm{e,n}}$ calculates like equation 1.12.

$$\varepsilon_{\mathrm{P}} = 1 - \frac{\omega_{\mathrm{P,e}}^2}{\omega\left(\omega - \mathbf{i}\nu_{\mathrm{e,n}}\right)} \qquad C_{\mathrm{p}} = \varepsilon_{\mathrm{p}} C_0 = \varepsilon_{\mathrm{p}} \varepsilon_0 \frac{A}{b} \tag{1.12}$$

$$Z_{\mathrm{P}} = \left(\mathbf{i}\omega C_{\mathrm{p}} + \frac{1}{\frac{1}{\omega_{\mathrm{P,e}}^2 C_0}\left(\nu_{\mathrm{e,n}} + \mathbf{i}\omega\right)} \right)^{-1} \tag{1.13}$$

The equation 1.13 represents the full impedance, consisting of the inverse sum of real and imagninary resitance, as well as the capacity of the neutral gas volume. Here, $\mathbf{i}\omega/(\omega_{\mathrm{p,e}}^2 C_0)$ characterizes the reaction of the electron movement to an external excitation of a frequency ω. The real part $\nu_{\mathrm{e,n}}/(\omega_{\mathrm{p,e}}^2 C_0$ denotes the charge current resistance by neutral particle collisions. For high excitation frequencies — a high frequency would be the mentioned 13,56 MHz — the bulk impedance can be neglected. Both the anodes and cathodes sheath capacity take the dominant part. Therefore, the discharge potential and voltage can be written as:

$$U(t) = U_{\mathrm{GS}} + U_{\mathrm{rf}} \sin(\omega t) \qquad \Phi_{\mathrm{P}}(t) = \overline{\Phi_{\mathrm{P}}} + \Phi_{\mathrm{rf}} \sin(\omega t) \tag{1.14}$$

1.1.5 Dielectric displacement current

1.1.6 Heating mechanisms

1.2 Negative ion physics

1.2.1 Anion creation and distribution

1.2.2 Dynamics and collisions

1.3 Particle-In-Cell simulations with Monte Carlo-Colissions

1.3.1 Principles

1.3.2 2d3v PIC

1.3.3 Monte Carlo-Collisions

Validation of Simulation by 1d comparison

2.1 Axial density profiles

2.2 Velocity and energy distributions

2.3 Transition to 2d simulation

Simulation of capacitively coupled rf discharges

3.1 Experimental setup

3.2 Secondary ion emission

3.3 Anion energy distributions in oxygen

Epilogue

4.1 Local electrostratic field solver

4.2 Diagnostics of current and charge

4.3 Field calculation

4.4 Comparison with Poisson-based solvers

Conclusion

Appendix

quantity	equation	relevance
Debye length	$\lambda_{\mathrm{D,j}}^2 = \frac{\varepsilon_0 k_\mathrm{B} T_\mathrm{j}}{n_\mathrm{j} e^2}$ $\lambda_\mathrm{D}^2 = \left(\lambda_{\mathrm{D,e}}^{-2} + \lambda_{\mathrm{D,i}}^{-2}\right)^{-1}$	distance around a charge, at which quasi-neutrality is satisfied,λ_D is the combined screening length from individual species
plasma parameter	$N_\mathrm{D} = n\frac{4}{3}\pi\lambda_\mathrm{D}^3$	number of particles inside Debye sphere, if $N_\mathrm{D} \gg 1$ an ionized gas is considered a plasma (degree of ionization)
plasma frequency	$\omega_{\mathrm{p,j}}^2 = \frac{n_\mathrm{j} e^2}{\varepsilon_0 m_\mathrm{j}} = \frac{v_{\mathrm{th,j}}}{\lambda_{\mathrm{D,j}}} = \frac{1}{\tau_\mathrm{j}}$	upper limit for interaction with fields/forces or external excitationsinverse screening time
thermal velocity	$v_{\mathrm{th,j}}^2 = \frac{k_\mathrm{B} T_\mathrm{j}}{m_\mathrm{j}}$	mean velocity from kinetic theory of gases
coulomb logarithm	$\ln(\Lambda)$ $\Lambda = \frac{b\,\mathrm{max}}{b\,\mathrm{min}} = \lambda_\mathrm{D} \cdot \frac{4\pi\varepsilon_0 \mu v_\mathrm{th}^2}{e^2}$	dimensionless scale for transport processes inside discharge fraction of probability for a cumulative 90° scattering by many small pertubation collisions and a single right angle scattering
collision frequency	$\nu_\mathrm{j} = \frac{e^4 n_\mathrm{j} \ln(\Lambda)}{8\sqrt{2m_\mathrm{j}}\pi\varepsilon_0 (k_\mathrm{B} T_\mathrm{j})^{3/2}}$	two body coulomb collision frequency inside species j
particle distance & mean free path	$\overline{b} = \frac{\hbar}{m_\mathrm{j} v_{\mathrm{th,j}}}$ $s_{\mathrm{mfp,j}} = \frac{v_{\mathrm{th,j}}}{\nu_{\mathrm{j,k}}}$	mean inter particle distance for species j free flight between subsequent collisions of species j and k with collision frequency $\nu_{\mathrm{j,k}}$

quantity	**equation**	**relevance**
speed of sound	$c_{\mathrm{S}}^2 = \frac{\gamma Z k_{\mathrm{B}} T_{\mathrm{e}}}{m_{\mathrm{i}}}$ $\gamma = 1 + 2/f = 5/3$	speed of longitudinal ion waves at electron pressure adiabatic coefficient with f, the kinetic degree of freedom
Debye-Hückel potential	$\Phi = \frac{Q}{4\pi\varepsilon\lvert\vec{r}\rvert} e^{-\frac{\lvert\vec{r}\rvert}{\lambda_{\mathrm{D}}}}$	electrostatic potential of charge particle Q at distance $\lvert\vec{r}\rvert$ equal to coulomb interaction with additional shielding by charged particles

Table A.1: Selection of physical properties of a low temperature ccrf discharge. The index j denotes the species, e.g. electrons, ions. Used quantities can be found in the preface in table 2.